UNIVERSITAT POLITÈCNICA
DE CATALUNYA
BARCELONATECH

UPCommons

Portal del coneixement obert de la UPC

http://upcommons.upc.edu/e-prints

© 2018. Aquesta versió està disponible sota la llicència CC-BY-NC-ND 4.0 http://creativecommons.org/licenses/by-nc-nd/4.0/

© 2018. This version is made available under the CC-BY-NC-ND 4.0 license http://creativecommons.org/licenses/by-nc-nd/4.0/

---

*Revised Manuscript - Clean Version
Click here to view linked References

Statistical modeling and mix design optimization of fly ash based engineered geopolymer composite using response surface methodology

Muhammad Zahid[a], Nasir Shafiq[b], M Hasnain Isa[c], Lluis Gil[d]

[a]PhD Scholar University Technology PETRONAS muhammadzahidutp@gmail.com
[b]Professor (Civil Engineering) University Technology PETRONAS nasirshafiq@utp.edu.my
[c]Associate Professor, University Technology PETRONAS Hasnain_isa@utp.edu.my
[d]Professor, Universitat Politècnica de Catalunya, lluis.gil@upc.edu

Abstract

Fly ash-based geopolymer binders have been identified as one of the alternatives to the Ordinary Portland Cement (OPC), which qualify the criteria of green construction material. In the process of enhancement of the properties of geopolymer; engineered geopolymer composite (EGC) is a recent development that is classified as the high-performance fiber reinforced geopolymer matrix. The philosophy of the development of EGC is to achieve high compressive strength and ductility. In this paper, statistical models are developed to predict the mechanical and post-cracking properties of EGC using Response Surface Methodology (RSM). In this regard, effects of three principal variables; molarity of sodium hydroxide, sodium silicate to sodium hydroxide ratio, and curing temperature on the properties of fresh and hardened EGC (setting time, compressive strength, elastic modulus, flexural strength, flexural toughness, ductility index, tensile strength, tensile first crack strength and tensile strain capacity) were investigated. All models are found significant because, and the difference between predicted R^2 and adjustable R^2 was found less than 0.2. The optimized mixture proportion was assessed using multi-objective optimization technique as discussed in the RSM literature. Finally, an experimental program was performed to validate the optimized mixture proportion. The predicted and experimental results were found in a close agreement because the variation between the predicted and the experimental results was obtained less than 5%. The proposed method can be performed for any objective value of the EGC property with desirability almost equal to one, improving the yield, the reliability of the product and the processes.

Keywords:

Geopolymer, Engineered Geopolymer Cement, NaOH molarity, Na_2SiO_3/NaOH Ratio, curing temperature, Response Surface Methodology (RSM), Optimization

1. Introduction

These days' aggressive campaigns are running around the world to promote the practices of sustainable living and the development and adaptation of carbon-friendly technologies. In developing a durable and green material or product, the fundamental principles are; limiting the utilization of natural resources and implementing an approach to reduction in the level of CO_2 emission. In the construction industry worldwide, ordinary Portland cement (OPC) is a widely used material (approximately 2 billion ton per annum at present and the demand is continuously increasing); cement manufacturing consumes a variety of raw materials mostly acquire from natural resources. Approximately 1.6 tons of natural raw material is used to produce one ton of OPC (Zahid et al., 2017). Because of the continual increase in the demand for cement-based materials; intense pressure is coming on the construction industry worldwide to develop alternative cementing materials in compliance with the sustainability and green material criteria. Since the beginning of this century; geopolymer (GP) binders are identified as the potential binding materials in producing green and sustainable concrete. GP binders are usually made of industrial byproducts called precursor (for example, fly ash) and can cause up to 70% reduction in CO_2 emission as compared to the use of OPC (McLellan et al., 2011). When precursors (rich in alumina and silica) are mixed with the alkaline solution and exposed to heat regime, the system undergoes to a continuous or in a chain reaction, and hence the cement-like binder material is formed, which is called geopolymer concrete (Zhuang et al., 2016). Fly ash the commonly used precursor is available abundantly, its annual production is more than 780 million tons, which is a byproduct of the coal-fired power stations around the globe (M. D.J. Sumajouw, 2006). Therefore, the use of fly ash as the principal constituent material of geopolymer resulted in a carbon-friendly binder without compromising on the mechanical and durability characteristics of concrete (Davidovits, 1991).

Since the inception of concrete as a structural material, it is well established that it is strong in resisting compression forces and weak in tension forces, furthermore, it exhibits low ultimate strain that made it a brittle material. To increase the ultimate strain level, to improve the ductility and to enhance the post-cracking behavior of concrete; fiber reinforced concrete (FRC) was introduced as one of the viable solutions. Addition of microfibers in FRC caton arrest the initial cracks usually induce in concrete at the early age, as a result of which an increase in the tensile

strength and ultimate strain level is achieved (Chen and Qiao, 2011). A common type of fibers is polyvinyl alcohol (PVA), polypropylene (PP), steel (ST), glass, asbestos, and basalt. All such fibers have shown many advantages and disadvantages when added in concrete. For example, due to low tensile strength and density of PP fibers, they did not show considerable improvement in the ultimate tensile and flexural strength of concrete (Horikoshi et al., 2005). Whereas, one of the weaknesses observed in the glass fibers is that they perform poorly in an alkaline environment (Horikoshi et al., 2005) and basalt fiber reinforced concrete exhibits softening behavior after the first crack appears (Choi and Lee, 2015). Similarly, steel fibers caused workability and dispersion issues in fresh concrete (Said and Abdul Razak, 2016). Based on several experimental investigations, PVA fibers are considered as a preferred type of fiber for producing high-performance FRC, because they possess a high modulus of elasticity and significant value of the tensile strength within the group of synthetic fibers. PVA fibers can also survive the alkaline environment. Salih et al. (2014) reported that PVA fibers improved mechanical properties and post-crack performance of concrete.

As reported in the literature that FRC has made significant improvements in enhancing the ultimate tensile strength, however, it does not perform well after initiation of the first cracks, or it softens once the first cracks appeared (Kim et. Al., 2008). Recent advancements in the research studies on FRC were mainly focused on increasing the post-cracking load carrying capacity of the structural members. When FRC mixes are modified to enhance the post-cracking load carrying capacity, such type of concrete is classified as the engineered cementitious composite (ECC). ECC usually contains maximum 2% volume fraction of randomly oriented microfibers based on the micromechanical design approach (VC Li, 1998). ECC structural members typically follow the multiple cracking behaviors that satisfy the steady-state crack opening condition (Yang and Li, 2007). Superior mechanical and excellent post crack properties of ECC include high compressive strength (30 to 80 MPa), a substantial value of ultimate strain (3-7%) and elastic modulus ranges from 10 to 25 GPa (Soe et al., 2013; VC Li, 1998).

There is insufficient research available in the literature on enhancing the characteristics and performance of fiber-reinforced geopolymer concrete (FRGPC). Ranjbar et al. (2016) reported that the addition of steel fibers had improved the flexural strength and the ductility of geopolymer concrete. Khan et al. (2018) investigated the mechanical properties of FRGPC by

using a hybrid combination an of steel and polyethylene fibers and observed an increase in the flexural and compressive strength. Introduction of engineered geopolymer composite (EGC) may be considered a new generation of fiber reinforced geopolymer concrete, which is designed to follow the similar pattern of achieving the mechanical and post-crack properties as that discussed for engineered cementitious composite (Nematollahi et al., 2015). The concentration of sodium hydroxide, NaOH/Na_2SiO_3 ratio, and curing temperature are identified as the most influencing parameters in achieving the mechanical properties of geopolymer concrete (Nuruddin et al., 2011). Compressive strength variation with the change in NaOH molarity and the Na_2SiO_3/NaOH ratio was investigated by the Mustafa Al Bakri et al. (2012) by fixing the curing condition at 70 ºC for a period of 24-hours. Geopolymer concrete mix prepared with Na_2SiO_3/NaOH of 2.5 12M NaOH solution showed highest compressive strength.

Owing to the multiple factors that influence the performance of geopolymer, it is essential to utilize the robust tool for the designing of EGC mix with less effort and limited usage of resources. Therefore, Response surface methodology (RSM), which is a powerful technique for the designing and analysis of different experiments in a systematic way. Finally, a model is developed to predict the output of the experiment. It includes the statistical approach for determining the relationship between independent input variables and dependent outputs (Eriksson et al., 1998). Furthermore, the best possible solution from the region of possible outcomes is selected for optimization (Anderson and Whitcomb, 1998). Advantages of utilizing RSM for designing the experiments include, a) less number of experiments b) development of a statistical model for desired output variables c) evaluation of the relationship between factors and response d) optimization of the responses for desired limitations (Upasani and Banga, 2004). RSM is widely accepted technique for the modeling and optimization of the experimental outputs in the OPC based concrete industry (Khayat et al., 2000). In their study, Cihan et al. (2013) used RSM to develop a statistical model for the six different variables as input and compressive strength of the ready-mix concrete as a response. Aldahdooh et al. (2013) utilized RSM to optimize the usage of OPC and silica fume content for the compressive strength of ultra-high performance fiber reinforced concrete. Mohammed et al.(2017), used RSM for the modeling and optimization of particular class of self-compacting PVA fiber reinforced composite. In their study, the effect of two variables (Nano silica content and fiber volume fraction) were investigated on the compressive strength, elastic modulus, and energy absorption.

Furthermore, the optimal proportions of each variable were suggested. Although RSM is successfully utilized for the modeling and optimization of OPC concrete, however, its introduction in the field of geopolymer technology is still novel. Gao et al. (2016) investigated and optimized the effect of concentration of alkali activator and liquid to solid ratio on the early compressive strength of the alkali-activated slag using RSM.

Therefore, the primary objective of the research work reported in this paper was to apply the RSM optimization technique in modeling the effects of principal variables (NaOH molarity, NaOH/Na_2SiO_3 and curing temperature) on the setting time, compressive strength, elastic modulus, first crack strength, flexural strength, flexural toughness and ductility index of the engineered geopolymer composites (EGC). To validate the optimum parameters obtained from the RSM output an experimental program was designed.

2. Experimental program

2.1. Material properties

In the present work, high calcium fly ash (HCFA) obtained from Manjung power plant, Perak, Malaysia. Micrograph of HCFA obtained from field emission scanning electron microscope (FESEM) is given in Figure 1. Elemental composition, loss on ignition (LOI) and surface area of HCFA was determined using X-ray fluorescence (XRF) and Brunauer Emmet Taller (BET) method; the relevant results are given in Table 1. It is well noted that CaO was more than 10% for HCFA. Further, the summation of SiO_2, Al_2O_3, and Fe_2O_3 was less than 70%. Hence the fly ash confirms the requirement of high calcium fly ash as per ASTM 618-10. Micro silica sand with a maximum particle size of 710µm and fineness modulus of 2.6 was used as aggregates.

Sodium hydroxide (NaOH) with 99% purity in combination with sodium silicate (Na_2SiO_3) was utilized as an alkaline solution to stimulate geopolymerization. The chemical composition of the alkaline solution is shown in table 2. Mechanical and physical properties of Polyvinyl alcohol (PVA) fiber are enlisted in Table 3.

2.2. Design of experiments using statistical response surface method

Response surface method (RSM) is a statistical approach uses for developing and validating the relationship between independent and dependent variables as factors and responses respectively.

The whole process comprises of four steps in total, which include, the design of experiments, a collection of response by performing experiments, development of RSM numerical model and optimization and validation of the developed model (Ghafari et al., 2014). Central composite design (CCD) is the most practical and commonly used method for design of experiments in RSM technique (Jose et al., 2014). As shown in Figure-2, CCD is a two-level factorial design; selection of data points include; corner points of the square for all +1 and -1 design points, a middle point between all factors, and star points having extreme $+\alpha$ and $-\alpha$ (Ferdosian and Camões, 2017).

Quadratic models are used to estimate the responses (compressive strength, elastic modulus, flexural strength, flexural toughness, ductility index, tensile strength and tensile strain), which are calculated according to the 2nd-degree polynomial equation 1 (Ghafari et al., 2014).

$$y = \beta_o + \sum \beta_i X_i + \sum \beta_{ii} {X_i}^2 + \sum \beta_{ij} X_i X_j \qquad (1)$$

Where "y" represents the predicted response, which may be mechanical characteristic (compressive strength, elastic modulus, flexural strength and tensile strength) and post-crack property (flexural toughness, ductility index, and tensile strain) of EGC. Furthermore, β_o, β_i, β_{ii} and β_{ij} are constant coefficient, linear coefficient, quadratic coefficient and interaction coefficient respectively. Moreover, X_i and X_j represent independent variables. Defined factors and their corresponding code, units, and levels are shown in Table 4.

The ranges of independent variables were selected based on literature review. Sodium hydroxide (NaOH) was varied from 8M to 16M whereas, Na_2SiO_3/NaOH ratio was ranged from 1 to 2.5 (Mustafa Al Bakri et al., 2012). Furthermore, curing temperature was kept constant to 24 hours with temperature range from 45 ºC to 90 ºC (Ali and Gupta, 2011). Other factors like sand to fly ash ratio, water to geopolymer solid ratio and PVA fiber volume fraction were kept constant at 0.3, 0.23 and 2% respectively (Nematollah et al. 2015). Commercially available, Design expert® software was used for the design of the experimental plan. As shown in Table 5, twenty mix designs of engineered geopolymer composite are randomly chosen according to the central composite design configurations for three factors with five center points.

2.3. Mixing and casting of Concrete

Geopolymer mortar mix proportions used in this experimental study are shown in Table-5, the principal aim of the study was to investigate the effect of NaOH molarity, curing temperature and Na_2SiO_3 on mechanical and post-crack properties of EGC. Mixing of GP mortar was done in Hobart mixture; in the beginning, fly ash and sand were dry mixed for thirty seconds in the slow mode then the alkaline solution was gradually added for next 30 seconds. In the final stage, PVA fibers were added in the matrix and mixed for four minutes at fast mode. After completion of the mixing process, the wet mixture was poured into the standard molds, which were kept in the laboratory until it hardened. After hardening of samples, they were taken out from the molds, and then the samples were tightly wrapped in plastic sheets to prevent excessive water lose during heat curing then the samples were placed in an oven at a specified temperature for 24 hours. After 24 hours of heat curing, all samples were stored in the lab at room temperature for 27 days.

3. Results and discussion

3.1. Workability and setting time of EGC

Workability of EGC was determined using mini-slump test as proposed by Nematollahi and Sanjayan, (2015). The slump flow of all EGC mixtures was obtained in the range of 250-300 mm; therefore, no vibration was applied during samples preparation. ECC is usually used for surface repairs and retrofitting of structures (Li et al., 2000). EGC synthesized with low calcium fly ash shows slow setting and could break while demolding even after one day of casting (Ohno and Li, 2014). On the other hand, HCFA based geopolymer can possess a flexible range of setting time with the variation of alkaline activator dosage and sodium silicate to sodium hydroxide ratios (Gomaa et al., 2017). Therefore, in this study, high calcium fly ash was used to synthesize EGC mixes. Initial and final setting time of EGC was conducted following ASTM C807-13. Variation in initial and final setting time was observed for different NaOH and Na_2SiO_3/NaOH ratio. Three-dimensional graphical representation of initial and final setting time is shown in Figure 3(a) and 4(a) respectively. Initial setting time was increased from 19 minutes to 40 minutes, with an increase in NaOH molarity and Na_2SiO_3/NaOH ratio from 4M to 16M and 1 to 2.5 respectively. It could happen, as the high dosage of alkaline medium curbs the leaching of calcium, hence, geopolymer gel (C-A-S-H) prevail over the calcium silicate hydrate gel (C-S-H) which results in longer setting time. Furthermore, the final setting time was increased with the decrease in Na_2SiO_3/NaOH ratio and increase in NaOH molarity. The lowest value of final setting time of 37

minutes was observed for the EGC mix synthesized with Na_2SiO_3/NaOH of 1.9 and 4M NaOH solution. Final setting time of 70 minutes was obtained as the peak final setting time, which was observed for the mixture made of Na_2SiO_3/NaOH of 1 and 16M NaOH. Intermittent values of initial and final setting time are shown in the contour shown in Figure 3(b) and 4(b) respectively. For the series of mixtures tested in this study, the initial and final setting times can be predicted from the ANOVA equations 2 and 3.

$$Initial\ setting\ time\ = +5.48433 + 0.57578\ * x_1 + 12.40293 * x_2 + 0.38889 * x_1 * x_2 - 0.031597 *\ {x_1}^2\ - 2.02222 * {x_2}^2 \quad (2)$$

$$Final\ setting\ time\ =\ +52.59666 + 3.83170 * x_1 - 28.91732x_2 * -0.50000\ *\ x_1 * x_2\ - 0.055903\ *\ {x_1}^2\ + 7.97778\ *\ {x_2}^2 \quad (3)$$

Where x_1 is NaOH molarity, and x_2 represents Na_2SiO_3/NaOH ratio.

3.2. Effects of NaOH molarity, Na_2SiO_3/NaOH ratio and curing temperature on the Compressive Strength

The compressive strength of concrete is an essential property for performing design of given structures, which is also valid for geopolymer binders. In geopolymers, compressive strength is primarily influenced by the concentration of the alkaline solution. Alkaline medium dissolve aluminosilicate source material to form gel structures, the said process is called gelation, further polymerization produces the geopolymer having the considerable compressive strength (Duxson et al., 2007). Usually, the Strong alkaline medium is necessary to promote the geopolymerization process. Various research studies identified that the curing temperature and the Na_2SiO_3/NaOH ratio also significantly influence the strength development of geopolymers (Hardjito et al., 2005). In this study, compressive strength development was investigated following ASTM C109/C109M − 16a. Results are plotted in the form of the 3D response surface, as shown in Figure 5 and 6. It is found that the compressive strength of the mixtures made of low molar was influenced more by varying curing temperature than the mixtures made of high molar solutions. In such mixtures (4M NaOH) a sharp reduction in compressive strength was observed when curing temperature was reduced from 90 ºC to 45 ºC. In case of mixtures made of 16M NaOH solution, the compressive strength with a change in curing temperatures didn't much difference.

It could be happened due to the presence of less-unreacted particles of source material in geopolymer with 16M NaOH as compared to that of 4M NaOH solution. Extended curing temperature from a certain level disrupts the granular morphology of geopolymer, consequently, decrease in compressive strength is observed (van Jaarsveld et al., 2002). Chindaprasirt et al., (2009) also reported that the increase in NaOH concentration causes a decrease in compressive strength after an absolute limit, which was also observed in this research study. It is recommended that the compressive strength of engineered cementitious composite(ECC) should be achieved within a range between 30 and 80 MPa (Mohammed et al., 2017). In a recent research Yu et. Al. (2017) Managed to achieve 100 MPa compressive strength of their ECC mixtures. In the current experimental study, the highest compressive strength of 91 MPa was obtained for engineered geopolymer composite (EGC) prepared using NaOH concentration of 10M, Na_2SiO_3/NaOH of 1.75 and curing temperature of 67.5 ºC.

In their study, Gao et al. (2016) investigated the effect of three parameters on the strength of alkali-activated slag (AAS). They utilized response surface methodology (RSM) for the optimization of mix design of AAS. Furthermore, RSM was validated by experimental results. It was observed that predicted values of compressive strength coincided with the experimental test results. Hence, they concluded that RSM accurately predicts the compressive strength. However, the compressive strength of EGC can be predicted using ANOVA equation 4.

$$Comp\ Strength = -69.90722 + 11.56527x_1 + 2.21019x_2 + 7.24578x_3 - 0.053167x_1x_2 + 0.65889x_1x_3 - 0.017630x_2x_3 - 0.34918x_1^2 - 0.00976990x_2^2 - 3.94373x_3^2 \quad (4)$$

Where x_1, x_2, and x_3 represents NaOH molarity, curing temperature and Na_2SiO_3/NaOH respectively

3.3. Effect of NaOH molarity, Na_2SiO_3/NaOH and curing temperature on the modulus of elasticity

Elastic modulus is important for describing the stiffness and the deformation capacity of the given material (Silva et al., 2016). The elastic modulus of EGC was determined according to ASTM C469/C469M− 14 standard. Due to the absence of coarse aggregates, ECC mixtures possess a low value of elastic modulus in comparison with conventional concrete (Zhang et al., 2015). In various research, similar behavior was reported for EGC. Figure 7 and 8 illustrate the

response surface and the contour for elastic modulus of EGC mixtures investigated in this research where Na_2SiO_3/NaOH ratio and NaOH molarity were the main parameters. It can be concluded that the increase in NaOH molarity and the curing temperature contributed to increasing the elastic modulus up to a certain limit then it decreased. However, Na_2SiO_3/NaOH ratio showed significant influence on establishing the elastic modulus of EGC mixtures with the high and low molar NaOH solution. Elastic modulus can be predicted by using ANOVA equation 5.

$$\text{Elastic modulus} = -10.60879 + 1.37862x_1 + 0.67028x_2 + 4.72127x_3 - 0.00962963x_1x_2 + 0.50000x_1x_3 + 0.038519x_2x_3 - 0.072953x_1^2 - 0.0042799x_2^2 - 1.05491x_3^2 \quad (5)$$

Where x_1, x_2 and x_3 represents NaOH molarity, curing temperature and Na_2SiO_3/NaOH respectively.

3.4. Flexural properties of EGC mixtures

3.4.1. Effects of NaOH molarity, Na_2SiO_3/NaOH ratio and curing temperature on flexural strength

Flexural strength test was performed according to the requirements of ASTM C78/C78M − 15b. Figure 8 and 9 shows response surface and contour diagrams for flexural strength against Na_2SiO_3/NaOH ratio and NaOH molarity. A statistical model was developed by Ghafari et al. (2014) for the flexural strength prediction. In their study, the effect of three independent variables (factors) was evaluated on the flexural strength of fiber reinforced concrete. The obtained model provides a reliable correlation between flexural strength and factors. Further, the multi-objective optimization technique was applied for getting highest flexural strength keeping the fiber content at a minimum. Validation of the optimized value of flexural strength was carried out by performing experiments. It was obtained that experimental value of flexural strength was in good agreement with the predicted one. Hence RSM was successfully utilized to predict and optimize the flexural strength of the fiber reinforced concrete. Similarly, for this research study, ANOVA model for the prediction of flexural strength (FS) of EGC is presented below in equation 6.

$$FS = -16.48784 + 0.79265x_1 + 0.55333x_2 + 5.28798x_3 - 0.00178704x_1x_2 + 0.071389x_1x_3 - 0.010593x_2x_3 - 0.043814x_1^2 - 0.00358710x_2^2 - 1.51562x_3^2 \quad (6)$$

Where x_1, x_2 and x_3 represents NaOH molarity, curing temperature and Na_2SiO_3/NaOH respectively.

3.4.2. Effect of NaOH molarity, Na_2SiO_3/NaOH ratio and curing temperature on flexural toughness

Flexural toughness is an important parameter that must be studied for investigating the structural performance of EGC; it is an indication of energy absorption capacity. The inclusion of fibers in concrete usually enhances its flexural toughness. Thus the material could be sufficiently tough to mitigate the hazardous dynamic loads, which can be caused by earthquake or blast (Naaman AE, 1995). Hence, structural engineers get useful information from flexural toughness for such applications. Flexural toughness is estimated by estimating the area under the load-deflection curve as defined by ASTM 1609/C1609M- 12. As shown in Figure 11, flexural toughness gently increased with the decrease in NaOH molarity. Furthermore, increase in flexural toughness was observed with the increase in the curing temperature up to a certain level, however, further increase in temperature caused a negative impact on the flexural toughness. It could be happened due to week fiber-matrix at elevated temperature. Effects of Na_2SiO_3/NaOH on the flexural toughness investigated in this study are shown in Figure 12. A regression model to estimate flexural toughness (FT) of EGC is demonstrated below in equation-7.

$$FT = -24.93230 + 0.73217x_1 + 1.09807x_2 + 8.12377x_3 - 0.00766667x_1x_2 + 0.38778x_1x_3 + 0.010667x_2x_3 - 0.074293x_1^2 - 0.00797181x_2^2 - 3.24626x_3^2 \quad (7)$$

3.4.3. Effects on ductility index

As shown in Figure 13, the gentle increment in ductility index was observed with the decrease in NaOH molarity. Furthermore, the highest value of ductility was observed at the moderate curing temperature. Moreover, Figure 14 represents the 3D response surface of ductility index the contour diagram, and it can be noticed that by increasing Na_2SiO_3/NaOH, the enhancement in ductility index was seen at higher molar NaOH solution. Furthermore, a slight increment followed by a decrease in ductility index was seen with increasing level of Na_2SiO_3/NaOH at the

lower molarity of NaOH solution. The ANOVA model to calculate the ductility index (DI) is presented in equation-8.

$$DI = -4.49110 - 2.63746x_1 + 1.04578x_2 + 15.87208x_3 + 0.021574x_1x_2 + 0.42500\,x_1x_3 + 0.068889x_2x_3 - 0.038175x_1^2 - 0.011165x_2^2 - 7.19184x_3^2 \quad (8)$$

3.5. Tensile properties of EGC mixtures

3.5.1. Effect of NaOH molarity, Na_2SiO_3/NaOH ratio and curing temperature on the ultimate tensile strength

Ultimate tensile strength was assessed by performing a direct tensile test on dog-bone shaped samples. Tensile load was applied at the constant rate of extension as 0.15 mm/s. The dog-bone shape is recommended by the Japanese Society of Civil Engineers (JSCE) for the determining of multiple cracking behaviors of high-performance concrete (Yokota et al., 1996). Figure 15 and 16 shows the response surface and contour diagrams of ultimate tensile strength influenced by the curing temperature, NaOH molarity, and Na_2SiO_3/NaOH ratio. In this study, the ultimate tensile strength of EGC mixtures was obtained in the range between 2MPa to 4.65 MPa and the ANOVA model to predict ultimate tensile strength (UTS) of EGC is given below in equation 9.

$$UTS = -4.00781 + 0.26838x_1 + 0.19993x_2 + 0.010123x_3 - 0.000601852x_1x_2 + 0.031944x_1x_3 + 0.00111111x_2x_3 - 0.015375x_1^2 - 0.00130287x_2^2 - 0.13550x_3^2 \quad (9)$$

3.5.2. Effects of NaOH molarity, Na_2SiO_3/NaOH and curing temperature on tensile strength with the first crack

First crack strength is necessary to estimate the projection of multiple cracking behaviors of EGC under direct tensile forces. Usually, in ECC, first crack strength is less than the ultimate tensile strength, and the region between them are considered as multiple cracking regions. For achieving the multiple cracking behaviors, first crack strength must be lower than the ultimate tensile strength (Yang et al., 2008). In the current study, all EGC mixture results showed multiple

cracking behaviors. The variation in the first crack strength was primarily affected by the change in the NaOH molarity, Na_2SiO_3/NaOH ratio, and the curing temperature. In Figure 17, Incremental change in the first crack strength can be observed with the change in NaOH molarity and increase in the curing temperature, and this behavior was implied to particular values of NaOH molarity and curing temperature. Figure 18 illustrates the decrease in first crack strength with the increase in Na_2SiO_3/NaOH ratio at the lowest NaOH concentration of 4M. The ANOVA model to predict the first tensile crack strength (FTCS) is given below in equation-10.

$$FTCS = -4.27969 + 0.39830x_1 + 0.17754\,x_2 - 0.95684x_3 - 0.00225926x_1x_2 + 0.11778x_1x_3 + 0.010815x_2x_3 - 0.020385\,x_1^2 - 0.00114928x_2^2 - 0.31153x_3^2 \quad (10)$$

3.5.3. Effect of NaOH molarity, Na_2SiO_3/NaOH and curing temperature on the Tensile Strain capacity

Tensile strain capacity of ECC is usually specified in the range of 3-7%, which is 300-700 times that of the normal concrete (Mohammed et al., 2017). In the current study, enhancement in tensile strain capacity of EGC mixtures was achieved with lower NaOH molarity and lower curing temperature as presented in Figure-19. Furthermore, as shown in Figure-20, Na_2SiO_3/NaOH ratio caused a variable effect on tensile strain capacity of EGC. For the tensile strain capacity (TSC) of EGC. ANOVA model is shown below in equation 11.

$$TSC = -1.00547 - 0.17567x_1 + 0.088434x_2 + 4.04299x_3 + 0.002x_1x_2 - 0.070556x_1x_3 + 0.00281481x_2x_3 - 0.000903670x_1^2 - 0.00100707x_2^2 - 0.96922x_3^2 \quad (11)$$

3.6. Validation of ANOVA Models

For the useful application ANOVA models established in this research and discussed in the previous sub-sections, they must be statistically validated. As presented in Table-6, the difference between predicted R^2 and adjusted R^2 for each response was less than 0.2, which can be defined that they are rationally in good agreement. Furthermore, adequate precision for all responses was greater than 4, which indicates the acceptance of developed model, so the models can satisfactorily be used to predict the response for the user-defined value of the desired factors. Analysis of variance (ANOVA) for full regression model of all responses is given in Table 7. A

higher magnitude of F-value and the smaller value of probability, which is less than 0.005 confirms the significance of the models (Subasi et al., 2016).

To avoid repetition, normal probability plot, predicted vs. actual plot and perturbation plot are shown only for compressive strength. Normal distribution of data is assessed with the help of graphical method named as normal probability plot. As shown in Figure 21, data points are approximately coincident with straight line hence data is normally distributed. Figure 22, depicts the predicted vs. actual plot. As the plot is almost 45-degree straight line, thus predicted values are in good agreement with actual values. For better understanding, the effect of NaOH molarity, Na_2SiO_3/NaOH and curing temperature on the compressive strength at a particular point, perturbation plot is shown in Figure 23. Steep slope given by factor, A (NaOH molarity) and B (curing temperature) indicates the sensitivity of both factors. However, a minor change in gradient was observed for factor C (Na_2SiO_3/NaOH) which is an indicator of a relatively less sensitive factor.

3.7. Optimization

It is difficult to get the optimal value of all individual responses within the same region. Hence, a multi-objective optimization is considered as the best solution to get the optimal solution, which satisfies the requirements of all responses concurrently. After developing and validating the ANOVA models for all the responses, multi-objective optimization technique was applied to find out the best possible responses. Global desirability function used for RSM optimization is given in equation 12 (Ferdosian and Camões, 2017).

$$D = (d_1^{r_1} * d_2^{r_2} * d_3^{r_3} * \dots * d_n^{r_n})^{1/\sum r_i} = [\int_{i=1}^{n} d_i^{r_i}]^{1/\sum r_i} \quad (12)$$

Where n is the number of independent variables (factors) as well as dependent variables (responses), which are included in the optimization process. In this research work, three independent variables namely NaOH molarity, curing temperature and Na_2SiO_3/NaOH ratio were used, in addition to that seven responses: compressive strength, elastic modulus, flexural strength, flexural toughness, ductility index, ultimate tensile strength and tensile strain capacity were optimized simultaneously. Where r_i is the importance of each of the factors or responses, the importance is rated at a scale from 1 to 5, and the number 1 shows the least importance

whereas the number 5 represents the highest importance. Individual desirability function represented by d_i ranged from 0 (non-desired) to 1 (desired). The geometric mean of the individual desirability of all variables (factors and responses) is considered as the desirability of the optimal solution. For desirability value close to one indicates that optimal solution is quite close to achieving the desired goal or target. The goal for responses (dependent variables) can be one of the given choices, such as "none," "maximize," "minimize," "target" or "in range," however, the desired goal for factor includes “equal to” instead of “none” choice. In the current study, compressive strength, elastic modulus, flexural strength, flexural toughness, ductility index, ultimate tensile strength and tensile strain capacity were "maximized," and all factors (NaOH molarity, curing temperature and Na_2SiO_3/NaOH) were kept in "in range." Graphical representation of the optimized EGC mix and corresponding optimal responses are shown in Figure 24. After getting the optimal solution, a validation study was carried out to find the variation in the results when obtained by performing experiments.

3.7.1. Experimental validation study

Considering the validation of ANOVA models, an experimentation program was conducted on the optimal mix conditions obtained from multi-objective optimization technique. All the experiments were performed following the methodology as described earlier. Figure-25 and 26 show flexural strength versus midspan deflection and ultimate tensile strength versus tensile strain capacity. Experimental results are found in good agreement with the predicted results with only 5% variation as shown in Table-8. Samples were able to achieve the desired deflection as well as strain hardening properties, in support of that Figure-27 is added as the evidence of multiple cracking behaviors executed in developed EGC matrix in this research study. w

4. Conclusion

In this study, RSM technique was used to establish the optimal mixing ratios for the engineered geopolymer composite (EGC) for the desired goal of responses. Principal conclusions drawn from this research study are given below:

1. The optimum conditions acquired from RSM can be employed for any given functional properties separately. The interaction of variables with the responses has been efficiently observed with the 3D surface diagrams. Ranges of variables for desired property can be

efficiently predicted from the intervals of various responses are given by the contour diagrams. Moreover, the desired responses can also be predicted by using ANOVA equations.

2. The RSM-ANOVA models of the compressive strength, elastic modulus, flexural strength, flexural toughness, ductility index, ultimate tensile strength, tensile first crack strength and tensile strain capacity for EGC have been developed and statistically validated.
3. The RSM can be used to design the experiment for EGC mixtures for any target value of response from the possible variable combination of factors. For example, the mix proportion of EGC for the compressive strength of 80 MPa can be estimated for the various molarity contents of NaOH, Na_2SiO_3/NaOH ratio and the curing temperature with the desirability approximately equal to 1.
4. The RSM optimization technique reduces the design time and improves the performance of the existing process and product, improves reliability and achieves robustness of the product and process.

References

Aldahdooh, M.A.A., Muhamad Bunnori, N., Megat Johari, M.A., 2013. Evaluation of ultra-high-performance-fiber reinforced concrete binder content using the response surface method. Mater. Des. 52, 957–965. https://doi.org/10.1016/j.matdes.2013.06.034

Ali MM, Gupta RS, Vanguri SV and Pahuja A., 2011. Investigations on curing conditions and properties of geopolymeric cements from coarser fly ash. Natl. Counc. Cem. Build. Mater. Ballabgarh, India.

Anderson, M.J., Whitcomb, P.J., 1998. Find the optimal formulation for mixtures. Chem. Eng. Prog. 2, 1–8.

Chen, Y., Qiao, P., 2011. Crack Growth Resistance of Hybrid Fiber-Reinforced Cement Matrix Composites. J. Aerosp. Eng. 24, 154–161. https://doi.org/10.1061/(ASCE)AS.1943-5525.0000031|10.1061/(ASCE)AS.1943-5525.0000031

Choi, J. Il, Lee, B.Y., 2015. Bonding properties of basalt fiber and strength reduction according to fiber orientation. Materials (Basel). 8, 6719–6727. https://doi.org/10.3390/ma8105335

Cihan, M.T., Güner, A., Yüzer, N., 2013. Response surfaces for compressive strength of concrete. Constr. Build. Mater. 40, 763–774. https://doi.org/10.1016/j.conbuildmat.2012.11.048

Davidovits J, 1991. Geopolymers: inorganic polymeric new materials. J. Therm. Anal. 1633–1656.

Duxson, P., Fernández-Jiménez, A., Provis, J.L., Lukey, G.C., Palomo, A., Van Deventer, J.S.J., 2007. Geopolymer technology: The current state of the art. J. Mater. Sci. 42, 2917–2933. https://doi.org/10.1007/s10853-006-0637-z

Eriksson, L., Johansson, E., Wikström, C., 1998. Mixture design - Design generation, PLS analysis, and model usage. Chemom. Intell. Lab. Syst. 43, 1–24. https://doi.org/10.1016/S0169-7439(98)00126-9

Ferdosian, I., Camões, A., 2017. Eco-efficient ultra-high performance concrete development by means of response surface methodology. Cem. Concr. Compos. 84, 146–156. https://doi.org/10.1016/j.cemconcomp.2017.08.019

Gao, Y., Xu, J., Luo, X., Zhu, J., Nie, L., 2016. Experiment research on mix design and early mechanical performance of alkali-activated slag using response surface methodology (RSM). Ceram. Int. 42, 11666–11673. https://doi.org/10.1016/j.ceramint.2016.04.076

Ghafari, E., Costa, H., Júlio, E., 2014. RSM-based model to predict the performance of self-compacting UHPC reinforced with hybrid steel micro-fiber. Constr. Build. Mater. 66, 375–383. https://doi.org/10.1016/j.conbuildmat.2014.05.064

Gomaa, E., Sargon, S., Kashosi, C., ElGawady, M., 2017. Fresh properties and compressive strength of high calcium alkali-activated fly ash mortar. J. King Saud Univ. - Eng. Sci. 29, 356–364. https://doi.org/10.1016/j.jksues.2017.06.001

Hardjito, D., Wallah, S.E., Sumajouw, D.M.J., Rangan, B.V., 2005. On the Development of Fly Ash-Based Geopolymer Concrete. ACI Mater. J. 467–472.

Horikoshi, T., Ogawa, a, Saito, T., Hoshiro, H., 2005. Properties of Polyvinylalcohol fibre reinforcing materials for cementitious composites. Int. Work. HPFRCC Struct. Appl. 2, 1–8.

Jose, J., Garcia-nieto, P.J., Alvarez-rabanal, F.P., Alonso-martínez, M., Dominguez-hernandez, J., Perez-bella, J.M., 2014. The use of response surface methodology to improve the thermal transmittance of lightweight concrete hollow bricks by FEM. Constr. Build. Mater. J. 52, 331–344. https://doi.org/10.1016/j.conbuildmat.2013.11.056

Khan, M.Z.N., Hao, Y., Hao, H., Shaikh, F.U.A., 2018. Mechanical properties of ambient cured high strength hybrid steel and synthetic fibers reinforced geopolymer composites. Cem. Concr. Compos. 85, 133–152. https://doi.org/10.1016/j.cemconcomp.2017.10.011

Khayat, K.H., Ghezal, A., Hadriche, M.S., 2000. Utility of statistical models in proportioning self-consolidating concrete. Mater. Struct. 33, 338–344. https://doi.org/10.1007/BF02479705

Li, V.C., Horii, H., Kabele, P., Kanda, T., Lim, Y.M., 2000. Repair and retrofit with engineered cementitious composites. Eng. Fract. Mech. 65, 317–334. https://doi.org/10.1016/S0013-7944(99)00117-4

McLellan, B.C., Williams, R.P., Lay, J., Van Riessen, A., Corder, G.D., 2011. Costs and carbon emissions for geopolymer pastes in comparison to ordinary Portland cement. J. Clean. Prod. 19, 1080–1090. https://doi.org/10.1016/j.jclepro.2011.02.010

Mohammed, B.S., Achara, B.E., Nuruddin, M.F., Y, M., Zulkefli, M.Z., 2017. Properties of nano-silica-modified self-compacting engineered cementitious composites. J. Clean. Prod. 162. https://doi.org/10.1016/j.jclepro.2017.06.137

Mustafa Al Bakri, A.M., Kamarudin, H., Bnhussain, M., Rafiza, A.R., Zarina, Y., 2012. Effect of Na2SiO3/NaOH ratios and NaOH molarities on compressive strength of fly-ash-based geopolymer. ACI Mater. J. 109, 503–508.

Naaman AE, R.H., 1995. Characterization of high-performance fiber reinforced cement composites. Proc. Second Int. RILEM Work. USA 1–24. https://doi.org/10.1520/C1609

Nematollahi, B., Sanjayan, J., 2015. Effect of different superplasticizer and activator combinations on workability and strength of fly ash based geopolymer. Elsevier 57, 667–672. https://doi.org/10.1016/j.matdes.2014.01.064

Nematollahi, B., Sanjayan, J., Shaikh, F.U.A., 2015. Matrix design of strain hardening fiber reinforced engineered geopolymer composite. Compos. Part B Eng. 27, 253–265. https://doi.org/10.1016/j.compositesb.2015.11.039

Nuruddin, M.F., Kusbiantoro, A., Qazi, S., Darmawan, M.S., Husin, N.A., 2011. Development of Geopolymer Concrete with Different Curing Conditions. IPTEK, J. Technol. Sci. 22, 24–28.

Ohno, M., Li, V.C., 2014. A feasibility study of strain hardening fiber reinforced fly ash-based geopolymer composites. Constr. Build. Mater. 57, 163–168. https://doi.org/10.1016/j.conbuildmat.2014.02.005

Ranjbar, N., Mehrali, M., Mehrali, M., Alengaram, U.J., Jumaat, M.Z., 2016. High tensile strength fly ash based geopolymer composite using copper coated micro steel fiber. Constr. Build. Mater. 112, 629–638. https://doi.org/10.1016/j.conbuildmat.2016.02.228

Said, S.H., Abdul Razak, H., 2016. Structural behavior of RC engineered cementitious composite (ECC) exterior beam-column joints under reversed cyclic loading. Constr. Build. Mater. 107, 226–234. https://doi.org/10.1016/j.conbuildmat.2016.01.001

Silva, R.V., De Brito, J., Dhir, R.K., 2016. Establishing a relationship between modulus of elasticity and compressive strength of recycled aggregate concrete. J. Clean. Prod. 112, 2171–2186. https://doi.org/10.1016/j.jclepro.2015.10.064

Subasi, A., Sahin, B., Kaymaz, I., 2016. Multi-objective optimization of a honeycomb heat sink using Response Surface Method. Int. J. Heat Mass Transf. 101, 295–302. https://doi.org/10.1016/j.ijheatmasstransfer.2016.05.012

Sumajouw MDJ, and Vijaya B., 2006. Low-Calcium Fly Ash-Based Geopolymer Concrete: Reinforced Beams and Columns. Concrete 1–120.

Upasani, R.S., Banga, A.K., 2004. Response surface methodology to investigate the iontophoretic delivery of tacrine hydrochloride. Pharm. Res. 21, 2293–2299. https://doi.org/10.1007/s11095-004-7682-6

van Jaarsveld, J.G.., van Deventer, J.S.., Lukey, G.., 2002. The effect of composition and temperature on the properties of fly ash- and kaolinite-based geopolymers. Chem. Eng. J. 89, 63–73. https://doi.org/10.1016/S1385-8947(02)00025-6

Yang, E.-H., Wang, S., Yang, Y., Li, V.C., 2008. Fiber Bridging Constitutive Law of Engineered Cementitious Composites. J. Adv. Concr. Technol. 6, 181–193. https://doi.org/10.3151/jact.6.181

Yokota, H., Rokugo, K., Sakata, N., 1996. JSCE Recommendations for Design and Construction of High-Performance Fiber Reinforced Cement Composite with Multiple Fine Cracks. High Perform. Fiber Reinf. Cem. Compos. 2 Proc. Int. Work.

Zahid, M., Shafiq, N., Nuruddin, M.F., Nikbakht, E., Jalal, A., 2017. Effect of Partial Replacement of Fly Ash by Metakaolin on Strength Development of Fly Ash Based Geopolymer Mortar, in Key Engineering Materials. Trans Tech Publications, Switzerland, pp. 131–135. https://doi.org/10.4028/www.scientific.net/KEM.744.131

Zhang, Z., Zhang, Q., Qian, S., Li, V.C., 2015. Low E Modulus Early Strength Engineered Cementitious Composites Material Development for Ultrathin Whitetopping Overlay. J. Transp. Res. Board 41–47. https://doi.org/10.3141/2481-06

Zhuang, X.Y., Chen, L., Komarneni, S., Zhou, C.H., Tong, D.S., Yang, H.M., Yu, W.H., Wang, H., 2016. Fly ash-based geopolymer: Clean production, properties, and applications. J. Clean. Prod. 125, 253–267. https://doi.org/10.1016/j.jclepro.2016.03.019.

Figure

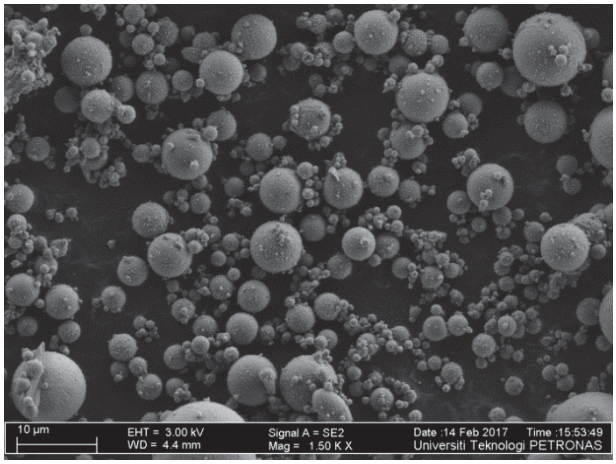

Figure 1. Micrographs of HCFA

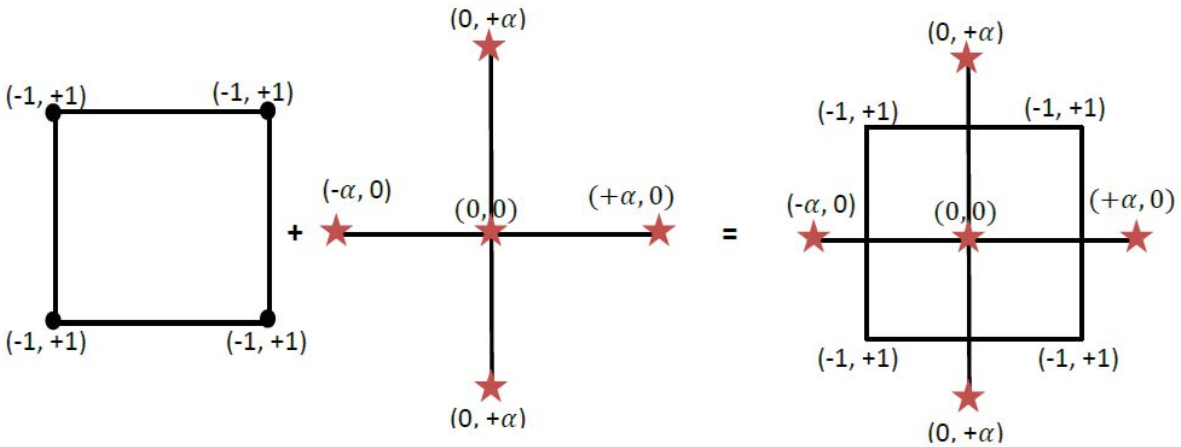

a) Corner points b) Middle point and extended central-point c) CCD design

Figure 2. Central composite design (CCD) module

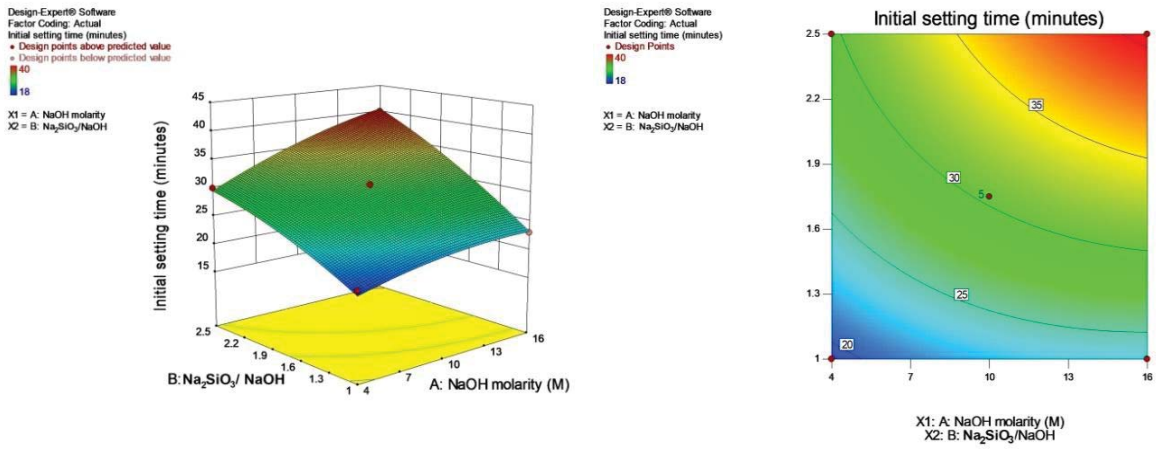

a) 3D response surface b) contour diagrams

Figure 3. Initial setting time versus Na_2SiO_3/NaOH and NaOH molarity

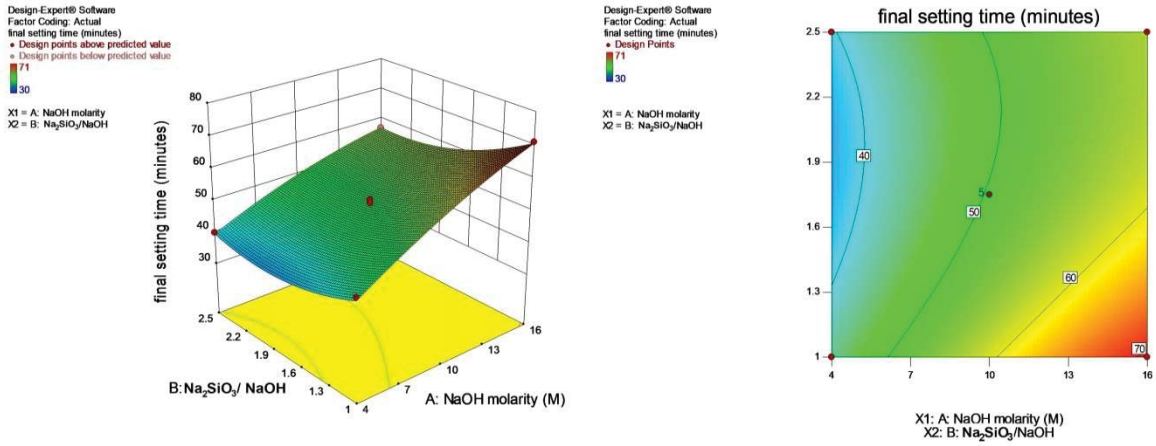

a) 3D response surface b) contour diagrams

Figure 4. Final setting time versus Na_2SiO_3/NaOH and NaOH molarity

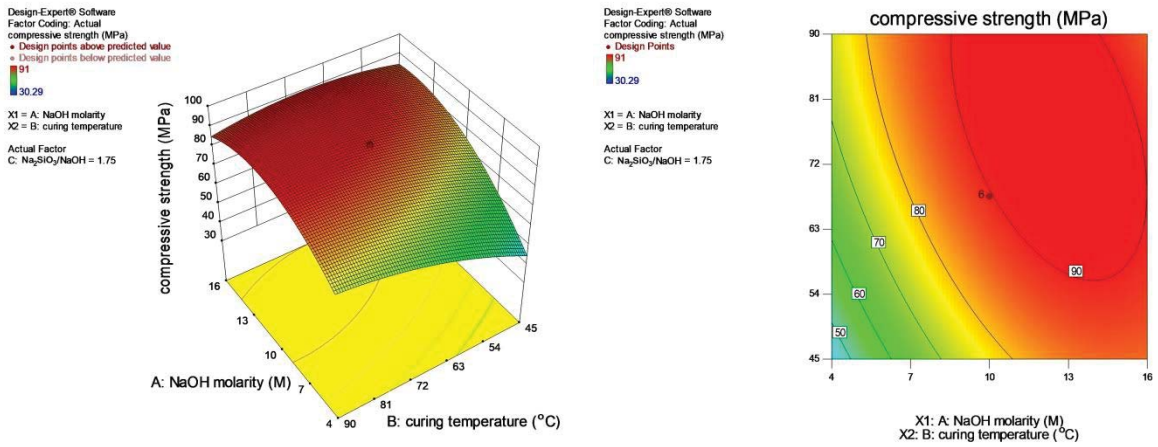

a) 3D response surface b) contour diagrams

Figure 5. Compressive strength versus curing temperature and NaOH molarity

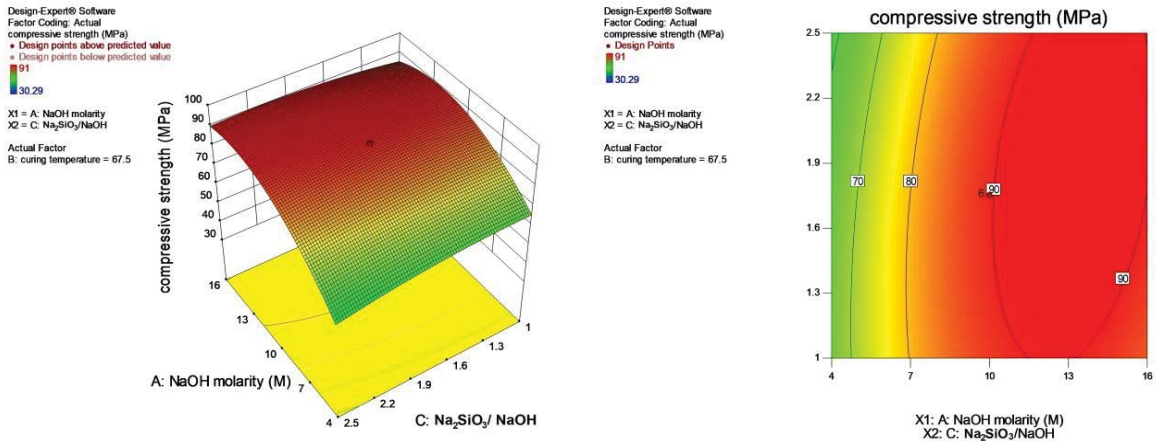

a) 3D response surface b) contour diagrams

Figure 6. Compressive strength versus Na_2SiO_3/NaOH and NaOH molarity

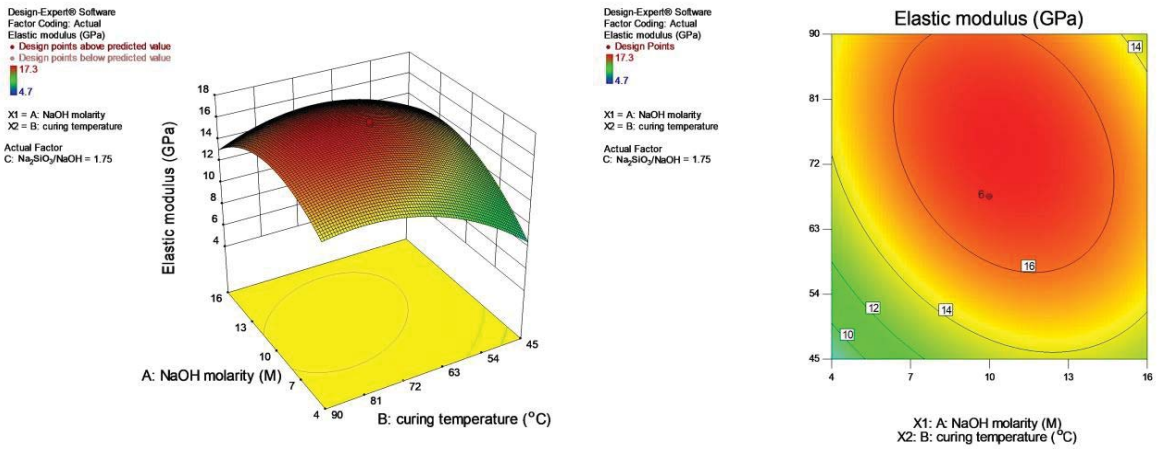

a) 3D response surface b) contour diagrams

Figure 7. Elastic modulus versus curing temperature and NaOH molarity

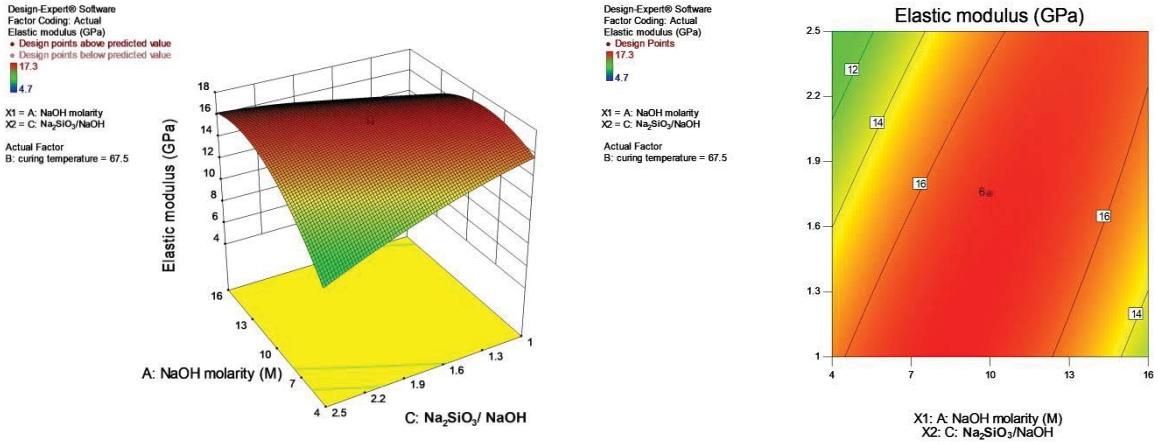

a) 3D response surface b) contour diagrams

Figure 8. Elastic modulus versus Na_2SiO_3/NaOH and NaOH molarity

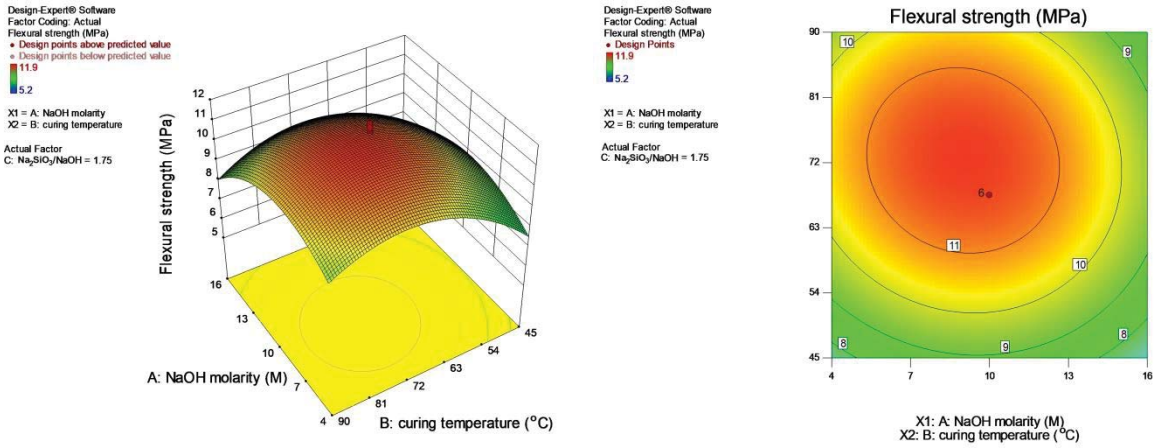

a) 3D response surface b) contour diagrams

Figure 9. Flexural strength versus curing temperature and NaOH molarity

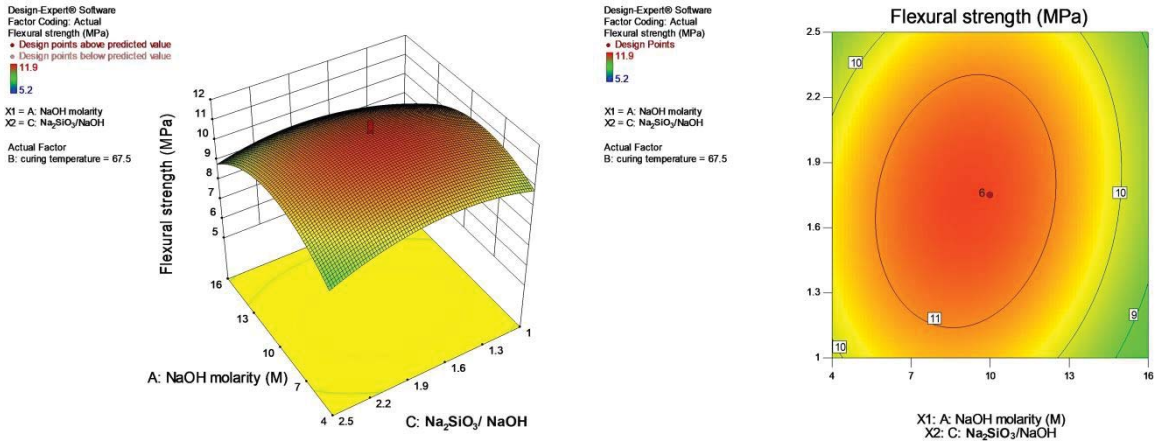

a) 3D response surface b) contour diagrams

Figure 10. Flexural strength versus Na_2SiO_3/NaOH and NaOH molarity

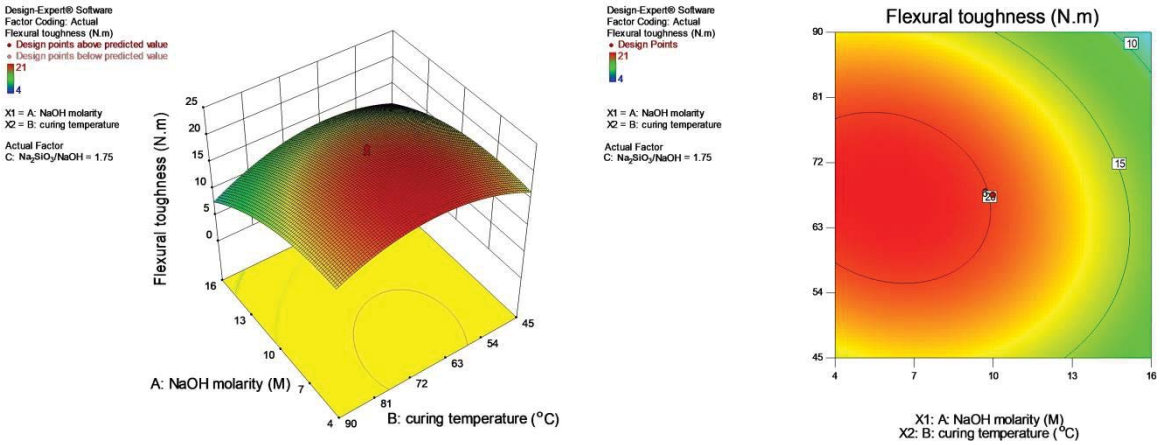

a) 3D response surface b) contour diagrams

Figure 11. Flexural toughness versus curing temperature and NaOH molarity

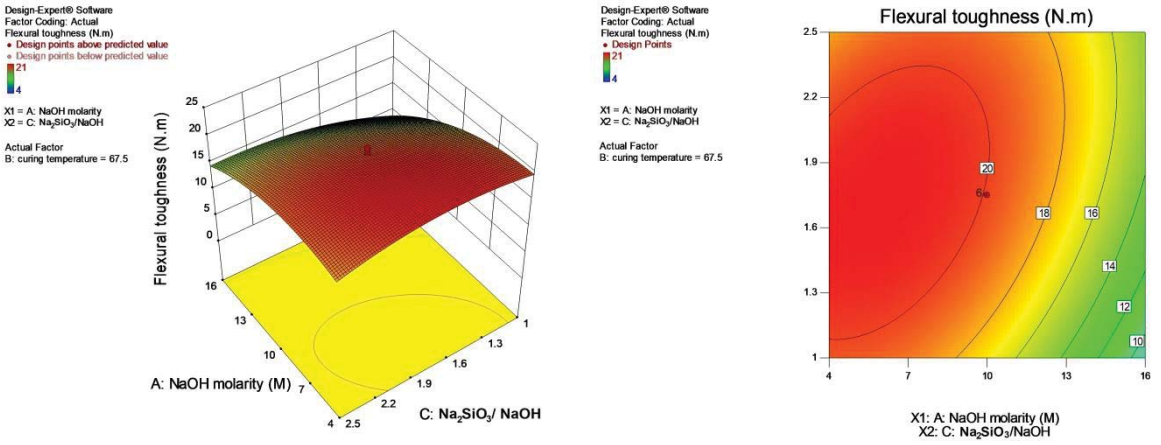

a) 3D response surface b) contour diagrams

Figure 12. Flexural toughness versus Na_2SiO_3/NaOH and NaOH molarity

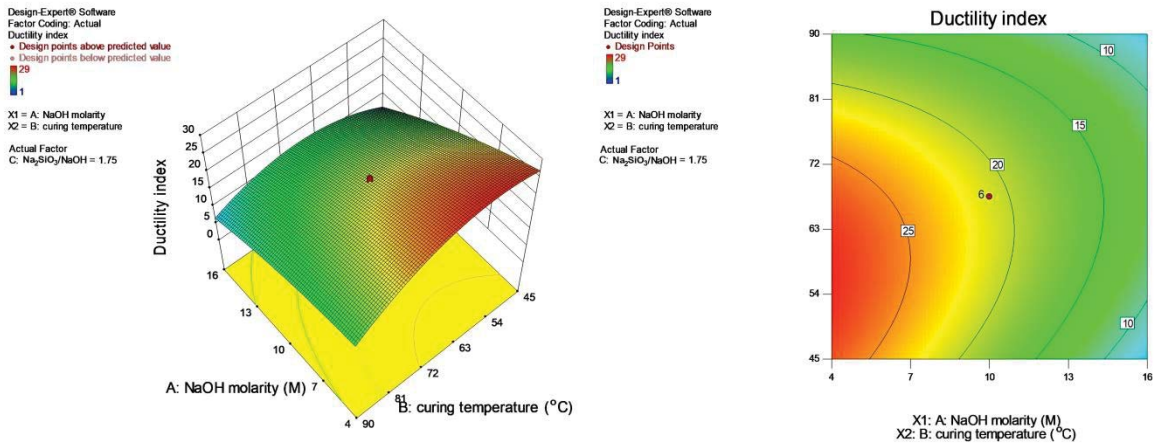

a) 3D response surface b) contour diagrams

Figure 13. Ductility index versus curing temperature and NaOH molarity

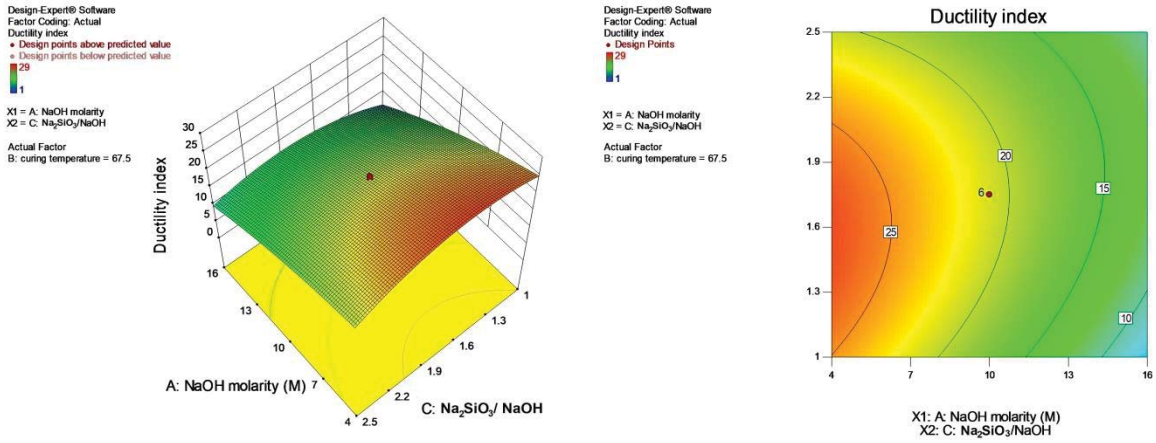

a) 3D response surface b) contour diagrams

Figure 14. Ductility index versus curing Na_2SiO_3/NaOH and NaOH molarity

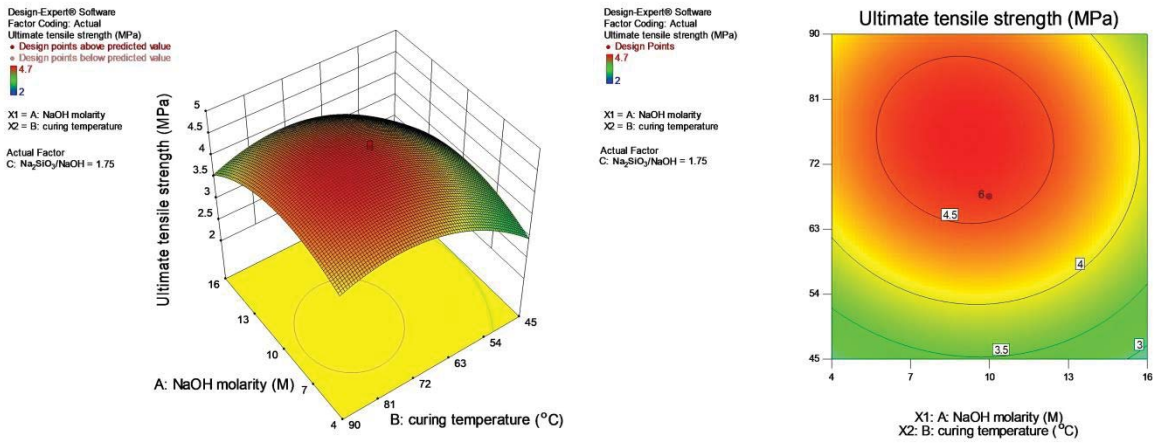

a) 3D response surface b) contour diagrams

Figure 15. Ultimate tensile strength versus curing temperature and NaOH molarity

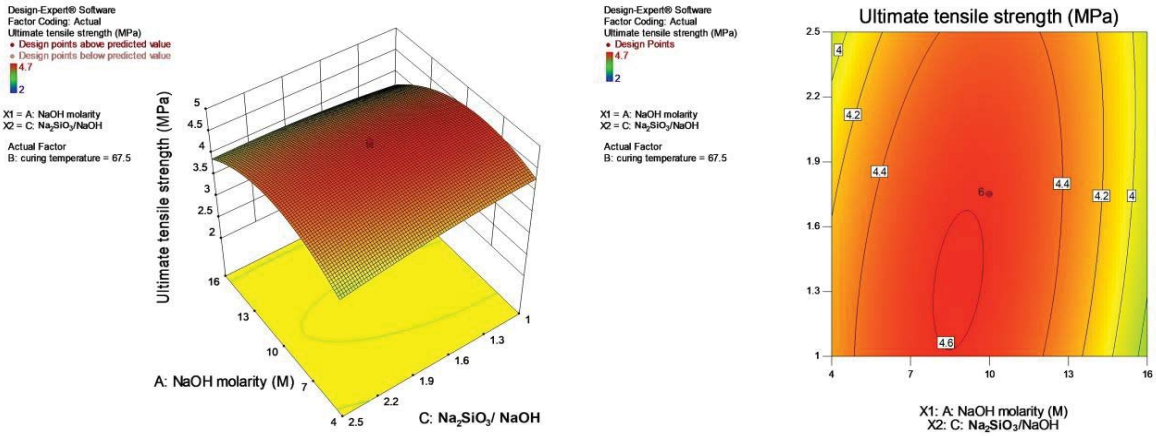

a) 3D response surface b) contour diagrams

Figure 16. Ultimate tensile strength versus Na_2SiO_3/NaOH and NaOH molarity

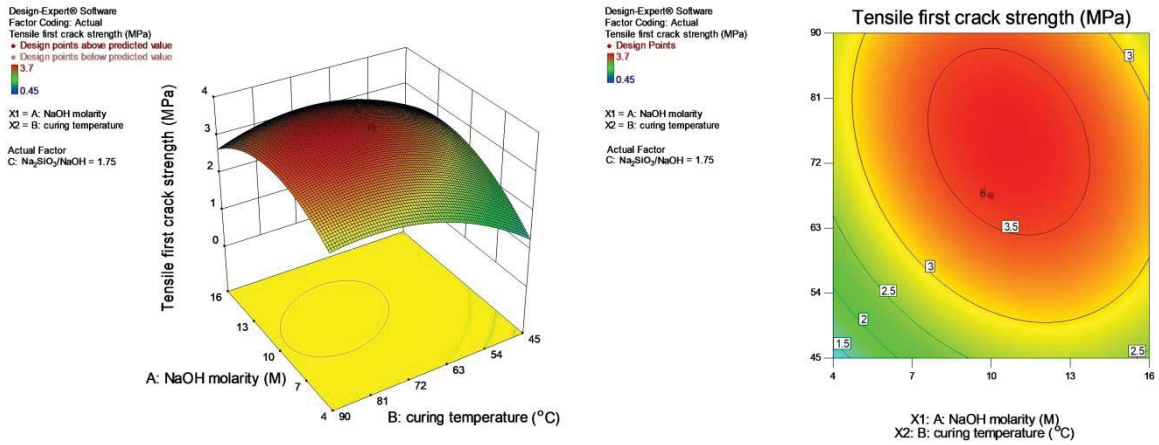

a) 3D response surface b) contour diagrams

Figure 17. Tensile strength after first crack versus curing temperature and NaOH molarity

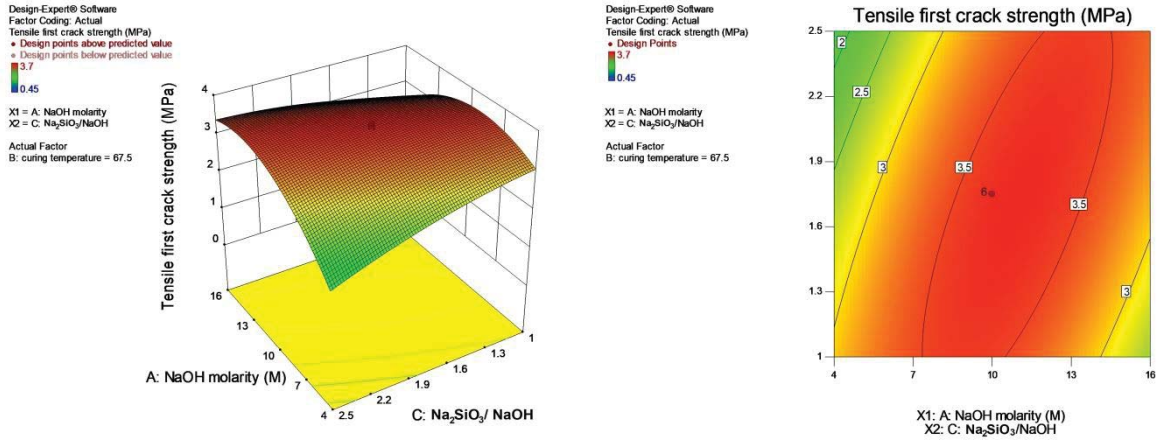

a) 3D response surface b) contour diagrams

Figure 18. Tensile first crack strength versus curing Na_2SiO_3/NaOH and NaOH molarity

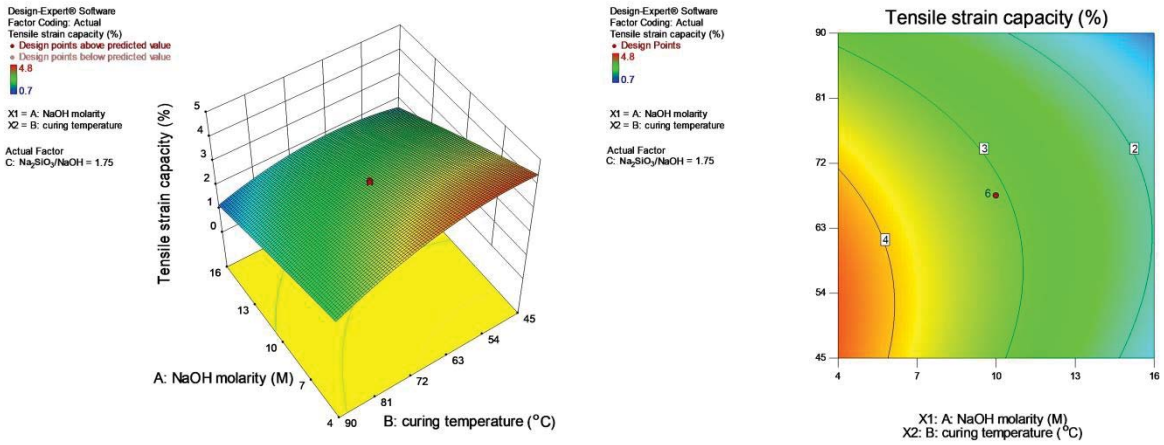

a) 3D response surface b) contour diagrams

Figure 19. Tensile strain capacity versus curing temperature and NaOH molarity

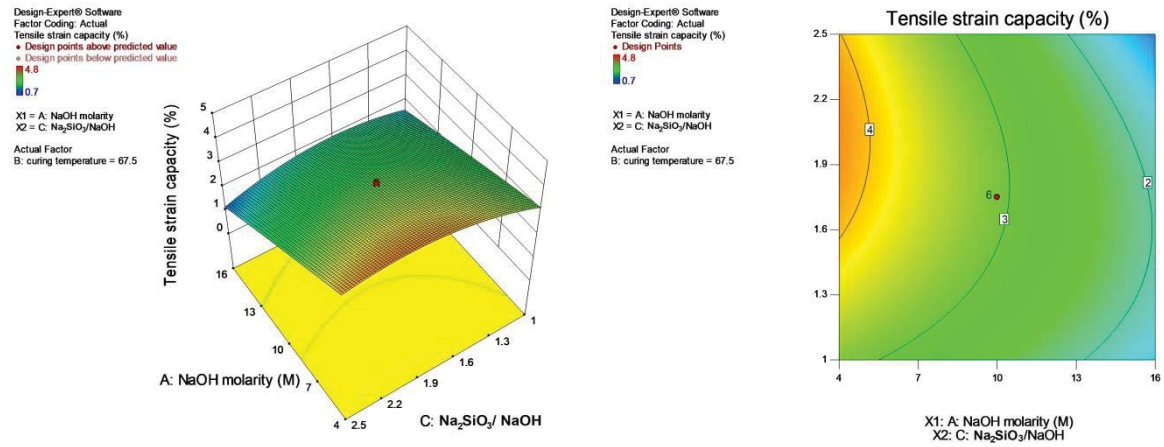

a) 3D response surface b) contour diagrams

Figure 20. Tensile strain capacity versus Na_2SiO_3/NaOH and NaOH molarity

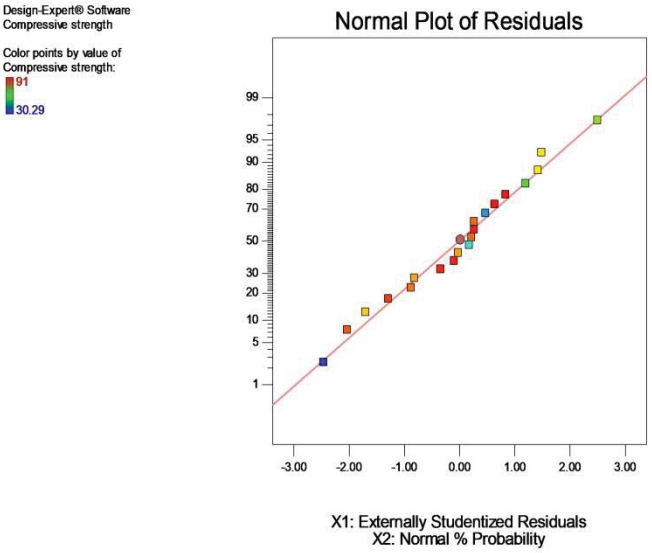

Figure 21. Normal plot of residuals for compressive strength

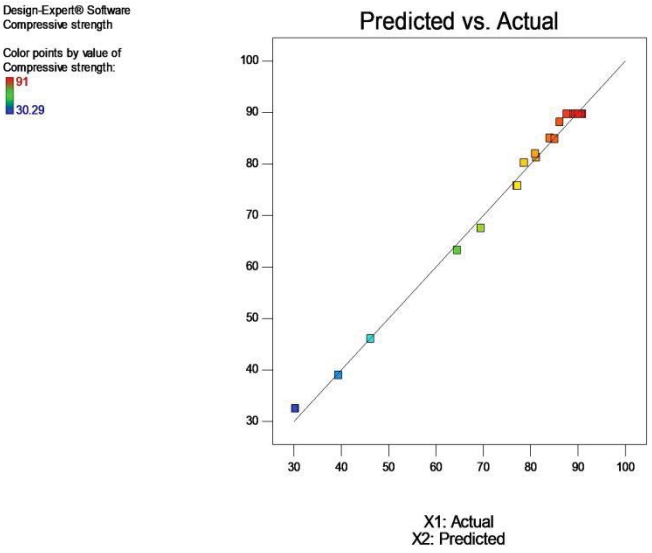

Figure 22. . Predicted vs actual for compressive strength

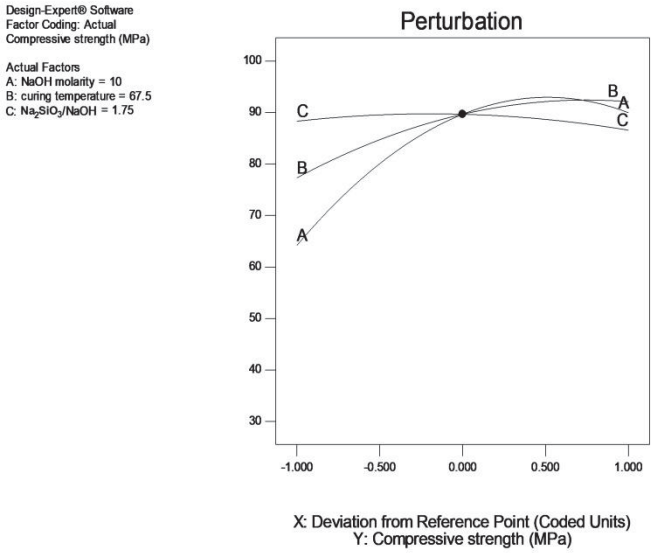

Figure 23. Perturbation curves for compressive strength

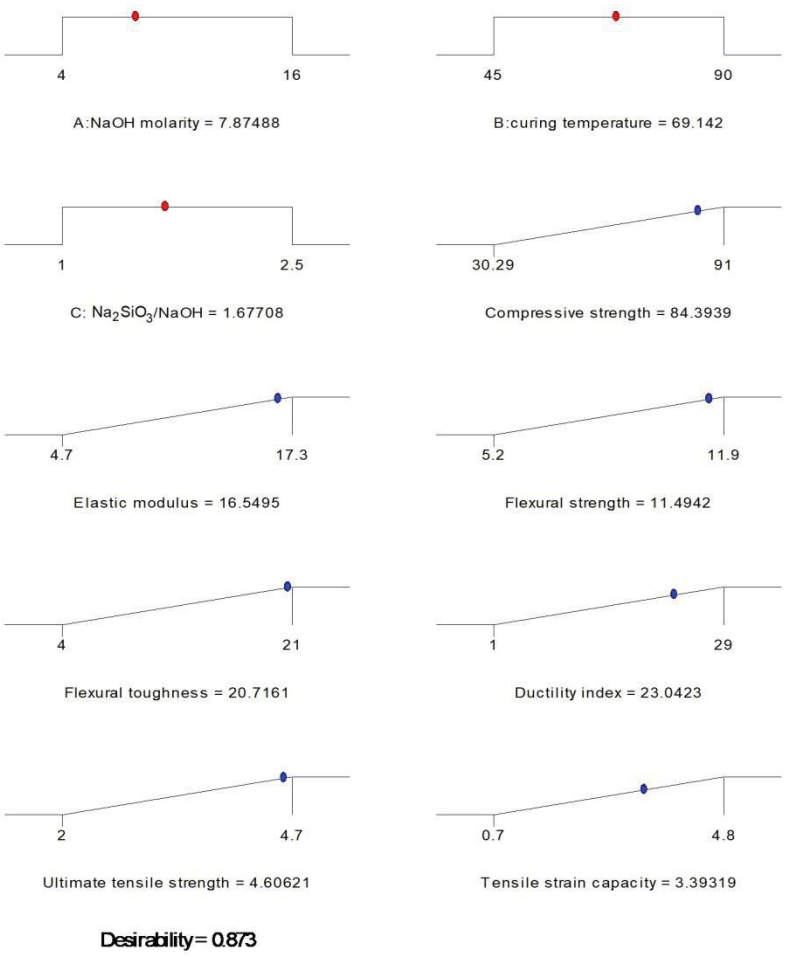

Figure 24. Ramps of optimized EGC

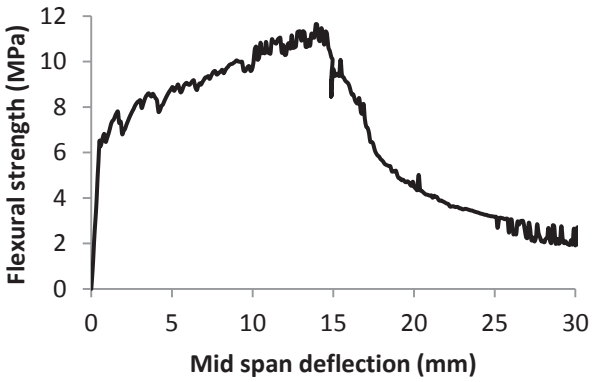

Figure 25. Flexural strength versus mid span deflection

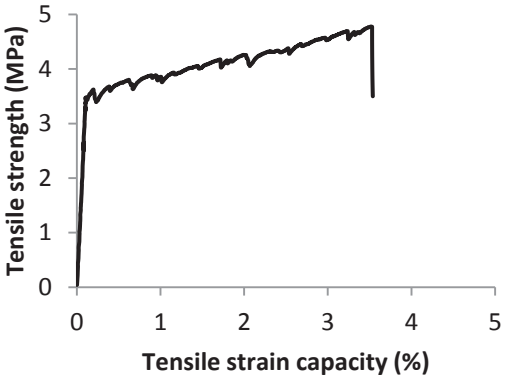

Figure 26. Tensile strength versus tensile strain capacity

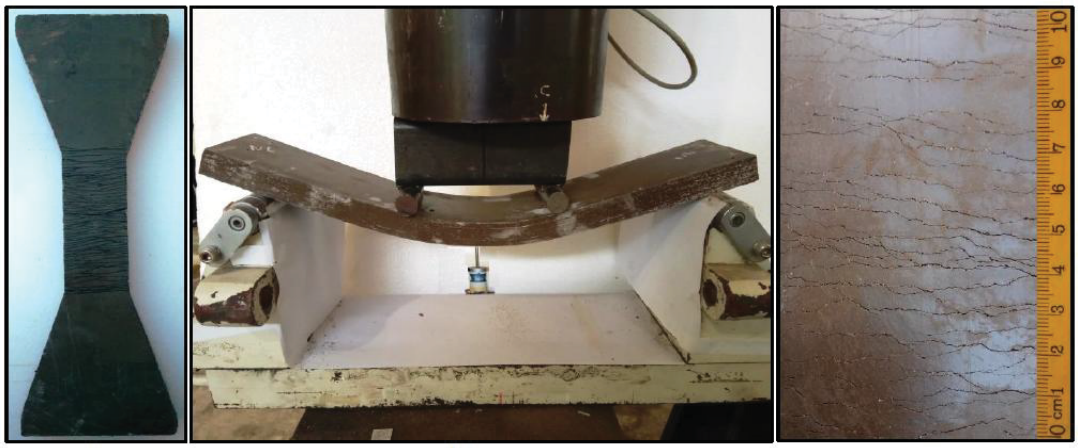

Figure 27. a) Multiple cracking under tensile stress, b) EGC deflection, c) Multiple cracking pattern

Table

Table 1. Elemental composition, loss on ignition (LOI) and surface area of HCFA obtained from XRF and BET method

Chemical composition of fly ash (%)										
SiO_2	Al_2O_3	Fe_2O_3	CaO	MgO	K_2O	SO_3	TiO_2	P_2O_5	LOI	BET (m^2/g)
35.5	12.73	23.6	19	2.27	2.1	1.5	1.46	1.2	0.6	0.9985

Note: LOI is loss on ignition and BET represents Average BET surface area

Table 2. Chemical composition of alkaline solution (% by mass)

Na_2SiO_3 solution (%)		4M NaOH solution (%)		10M NaOH solution (%)		16M NaOH solution (%)		20M NaOH solution (%)	
Na_2O	14.7	NaOH	15	NaOH	33	NaOH	48	NaOH	59
SiO_2	29.75	H_2O	85	H_2O	67	H_2O	52	H_2O	41
H_2O	55.52								

Table 3. Properties of micro PVA fiber

Brand	Product code	Length (mm)	Diameter (mm)	Fiber strength (MPa)	Youngs modulus (GPa)	Elongation (%)	Density (g/cm^3)
Kuraray	RECS 15	8	0.04	1600	41	6	1.3

Note: The type of PVA fiber is chosen from available literature (Nematollahi et al., 2015)

Table 4. Boundaries of factors in RSM

Factor	code	units	levels				
			$-\alpha$	-1	0	+1	$+\alpha$
NaOH molarity	X_1	M	0	4	10	16	20
Curing temperature	X_2	ºC	30	45	67.5	90	105
$Na_2Sio_3/NaOH$	X_3	-	0.48	1	1.75	2.5	3

Table 5. Experimental mix designs of EGC

Run	Factor 1 NaOH molarity M	Factor 2 Curing temperature °C	Factor 3 Na_2SiO_3/ NaOH	Alkaline solution[a]	Extra water[a]	Water/ Geopolymer solids[a]	Fly ash	Sand[a]	PVA Fiber[b]
1	10	105	1.75	0.36	0.054	0.23	1	0.3	0.02
2	10	67.5	0.48	0.36	0.039	0.23	1	0.3	0.02
3	20	67.5	1.75	0.36	0.096	0.23	1	0.3	0.02
4	4	90	2.5	0.36	0.035	0.23	1	0.3	0.02
5	10	67.5	1.75	0.36	0.054	0.23	1	0.3	0.02
6	10	67.5	1.75	0.36	0.054	0.23	1	0.3	0.02
7	4	45	1	0.36	0.007	0.23	1	0.3	0.02
8	16	45	1	0.36	0.081	0.23	1	0.3	0.02
9	16	45	2.5	0.36	0.077	0.23	1	0.3	0.02
10	4	45	2.5	0.36	0.035	0.23	1	0.3	0.02
11	10	67.5	1.75	0.36	0.054	0.23	1	0.3	0.02
12	10	67.5	1.75	0.36	0.054	0.23	1	0.3	0.02
13	4	90	1	0.36	0.007	0.23	1	0.3	0.02
14	10	30	1.75	0.36	0.054	0.23	1	0.3	0.02
15	0	67.5	1.75	0.36	0	0.23	1	0.3	0.02
16	16	90	1	0.36	0.081	0.23	1	0.3	0.02
17	10	67.5	1.75	0.36	0.054	0.23	1	0.3	0.02
18	10	67.5	3	0.36	0.060	0.23	1	0.3	0.02
19	16	90	2.5	0.36	0.077	0.23	1	0.3	0.02
20	10	67.5	1.75	0.36	0.054	0.23	1	0.3	0.02

Note: Dosage of Fly ash, sand, PVA fiber and Water/Geopolymer solids is selected from available literature (Nematollahi et al., 2015). Extra water is added to make water to geopolymer solids ratio constant (if needed). Geopolymer solids (solids in NaOH and Na_2SiO_3 solution plus fly ash). For run 15, NaOH molarity of "0" represents tap water without NaOH pallets.

[a] Quantity in mass ratio of fly ash

[b] Quantity in volume fraction of the total volume of material

Table 6. Model validation for responses

Response	Compressive strength (MPa)	Elastic modulus (GPa)	Flexural strength (MPa)	Flexural toughness (N.m)	Ductility index	Tensile first crack strength (MPa)	Ultimate tensile strength (MPa)	Tensile strain capacity (%)
Standard deviation	1.72	0.24	0.27	0.96	1.99	0.15	0.17	0.21
Mean	76.19	13.26	8.57	14.07	13.36	2.58	3.70	2.34
R^2	0.9951	0.9977	0.9924	0.9837	0.9731	0.9876	0.9791	0.9850
Predicted R^2	0.9699	0.9879	0.9697	0.8800	0.8109	0.9081	0.8530	0.8889
Adjusted R^2	0.9906	0.9956	0.9856	0.9690	0.9531	0.9764	0.9603	0.9715
Adequate precision	46.959	72.835	33.942	24.745	20.732	30.728	22.218	29.291

Table 7. ANOVA results for full regression model of each response

Response	Compressive strength (MPa)	Elastic modulus (GPa)	Flexural strength (MPa)	Flexural toughness (N.m)	Ductility index	Tensile first crack strength (MPa)	Ultimate tensile strength (MPa)	Tensile strain capacity (%)
Sum of squares	5987.04	253.38	92.33	560.87	1567.40	18.37	13.05	28.76
Mean square	665.23	28.15	10.26	62.32	174.16	2.04	1.45	3.20
F-value	224.1	478.31	145.52	66.93	43.93	88.51	52.08	72.98
p-value prob > F	< 0.0001	< 0.0001	< 0.0001	< 0.0001	< 0.0001	< 0.0001	< 0.0001	< 0.0001
Remarks	significant	significant	significant	significant	significant	significant	significant	significant

Table 8. Response results of the experiment and prediction model for optimal mix design

Response	Compressive strength (MPa)	Elastic modulus (GPa)	Flexural strength (MPa)	Flexural toughness (N.m)	Ductility index	Ultimate tensile strength (MPa)	Tensile strain capacity (%)
Predicted	84.39	16.55	11.49	20.71	23.04	4.60	3.39
Experimental	81.23	15.78	10.94	21.24	22.17	4.42	3.24
Error (%)	3.74	4.65	4.78	2.56	3.77	3.91	4.42